

Supporting Information

**Two Novel Aromatic Hydrocarbons: Facile Synthesis, Photophysical Properties and Applications in Deep-Blue Electroluminescence**

Zhixiang Gao<sup>a</sup>, Yuling Wu<sup>b,\*</sup>, Wenshan Qu<sup>a</sup>, Tianbao Li<sup>b</sup>, Tingting Yang<sup>a</sup>, Xiaxia Fan<sup>a</sup>, Lijuan Dong<sup>a</sup>, Yunlong Shi<sup>a</sup>, Xuerui Cheng<sup>c</sup>, Yufen Ren<sup>c</sup>, and Peng Tao<sup>b,\*</sup>

<sup>a</sup> School of Physics and Electronic Science, Shanxi Datong University, Datong, 037009, P. R. China

<sup>b</sup> Key Laboratory of Interface Science and Engineering in Advanced Materials, Ministry of Education, Taiyuan University of Technology, Taiyuan, 030024, China

<sup>c</sup> Department of Technology and Physics, Zhengzhou University of Light Industry, Zhengzhou, 450002, P. R. China

Corresponding E-mail: wuyuling@tyut.edu.cn (Y. Wu); iamtaopeng@gmail.com (P. Tao).

## 1. General Experimental Information

All operations were performed under an inert nitrogen atmosphere using standard Schlenk unless otherwise stated. All solvents were used after distillation and stored over activated molecular sieves (5 Å). All reagents and chemicals were purchased from commercial sources and used without further purification. The NMR spectra were recorded with a Bruker spectrometer at ambient temperature. Mass spectrum was obtained on SHIMADZU matrix-assisted laser desorption/ionization time-of-flight mass spectrometer (MALDI-TOF-MASS). Elemental analyses were carried out with a VarioEL III O-Element Analyzer system. The UV-vis absorption spectrum was recorded on a Shimadzu UV-2550 spectrometer. Steady-state emission experiments at room temperature were measured on an Edinburgh LFS-920 spectrometer. Excited-state lifetime studies were performed with an Edinburgh LFS-920 spectrometer with a hydrogen-filled excitation source. The data were analyzed by a software package provided by Edinburgh Instruments. The absolute quantum yields of the complex was determined through an absolute method by employing an integrating sphere. Cyclic voltammetry measurements were carried out in CH<sub>2</sub>Cl<sub>2</sub> (5×10<sup>-4</sup> M) with a three-electrode cell configuration consisting of platinum working and counter electrodes and a Ag/AgNO<sub>3</sub> (0.01 M in CH<sub>3</sub>CN) reference electrode at room temperature. Tetra-*n*-butylammonium hexafluorophosphate (0.1 M in CH<sub>2</sub>Cl<sub>2</sub>) was used as the supporting electrolyte. The redox potentials were recorded at a scan rate of 100 mV/s and are reported with reference to the ferrocene/ferrocenium (Fc/Fc<sup>+</sup>) redox couple.

## 2. EL Device Fabrication and Testing

The devices were fabricated on pre-patterned ITO glass substrates with a sheet resistance of 15Ω/square. The ITO glass substrates were sequentially cleaned by the detergent, acetone, isopropyl alcohol and deionized water before use. Prior to the thin film deposition, the substrates were treated with the UV ozone to improve the work function and also to remove the possible chemical residuals left on the ITO surface during the wet cleaning processes. Poly(3,4-ethylenedioxythiophene) doped with

poly(styrenesulfonate) (PEDOT:PSS) were spin-coated onto the cleaned ITO substrates at 3000 rpm for 40 s, and annealed for 20 min at 120 °C. The poly(9-vinylcarbazole) (PVK) layer was prepared by spin-coating (PVK in chlorobenzene (5 mg/mL)) at 3000 rpm for 40 s, and annealed for 10 min at 100 °C in the glove box. The thickness of the PVK is about 20 nm. The EML layer was prepared by spin-coating (compound **1** in toluene (5 mg/mL)) at 3000 rpm for 40 s, and annealed for 10 min at 100 °C in the glove box. The thickness of the EML is about 20 nm. Afterwards, the ITO glass substrates with PVK layer and EML layer were loaded in a vacuum chamber for deposition of organic layers using thermal evaporation under a base pressure of  $5 \times 10^{-4}$  Pa. The film thicknesses and the corresponding deposition rates were controlled by the calibrated crystal quartz sensors. Deposition rates of functional organic layers, the cathode interlayer LiF and the top Al contact were about 1 Å/s, 0.1 Å/s and 3-6 Å/s, respectively. The active emissive area of the devices is 3 mm × 3 mm, defined by the overlap between ITO anode and Al cathode.

The EL spectra, CIE coordinates of OLEDs were measured using a computer controlled PR-655 spectra scan spectrometer. The *J-V-L* was measured by a computer-controlled Keithley 2400 source meter integrated with a BM-70A luminance meter. The *CE* and *PE* were calculated from the plot of *J-V-L*. The *EQE* was calculated from the *J-V-L* curve and spectra data. All samples were characterized immediately after thin films deposition without encapsulation.

### 3. Synthesis of **1** and **2**

**1,4-bis(9,9-dihexyl-9H-fluoren-2-yl)naphthalene (1).** 2-(9,9-Dihexyl-9H-fluoren-2-yl)-4,4,5,5-tetramethyl-1,3,2-dioxaborolane (0.6 mmol), 1,4-dibromonaphthalene (0.3 mmol) and Pd(PPh<sub>3</sub>)<sub>4</sub> (0.03 mmol) was added to mixtures of ethanol (15 mL), toluene (50 mL), and 2.0 M K<sub>2</sub>CO<sub>3</sub> aqueous solution (20 mL). The mixtures were stirred at 85

°C for 24 h under N<sub>2</sub>. After the reaction was finished, the mixtures were diluted with CH<sub>2</sub>Cl<sub>2</sub> and washed with water, dried over anhydrous Na<sub>2</sub>CO<sub>3</sub>, then the solvent evaporated. The crude product was purified by column chromatography to give white powder (petroleum ether as the eluent) (85% Yield). <sup>1</sup>H NMR (400 MHz, CDCl<sub>3</sub>, δ): 8.06 (dd, *J* = 6.5, 3.3 Hz, 2H), 7.87 (d, *J* = 8.1 Hz, 2H), 7.80 (d, *J* = 7.2 Hz, 2H), 7.61 (s, 2H), 7.55 (d, *J* = 5.7 Hz, 4H), 7.46 (dd, *J* = 6.6, 3.3 Hz, 2H), 7.37 (dq, *J* = 9.5, 6.2 Hz, 6H), 2.10-1.97 (m, 8H), 1.23-1.05 (m, 25H), 0.82-0.78 (m, 21H). <sup>13</sup>C{<sup>1</sup>H} NMR (100 MHz, CDCl<sub>3</sub>, δ): 151.14, 150.86, 141.02, 140.51, 140.48, 139.67, 132.44, 128.91, 127.27, 127.01, 126.70, 126.65, 125.93, 125.10, 123.03, 119.94, 119.74, 55.30, 40.57, 31.69, 29.89, 24.05, 22.74, 14.19. Anal. calcd for C<sub>60</sub>H<sub>72</sub>: C, 90.85; H, 9.15; found: C 90.89, H 9.20. MALDI-TOF-MS (*m/z*): calcd for C<sub>60</sub>H<sub>72</sub>, 792.563; found, 792.562.

**1,5-bis(9,9-dihexyl-9H-fluoren-2-yl)naphthalene (2).** This compound was obtained in the yield of 90% by the same procedure as the compound **1**. <sup>1</sup>H NMR (400 MHz, CDCl<sub>3</sub>, δ): 8.00 (d, *J* = 8.4 Hz, 2H), 7.87 (d, *J* = 8.1 Hz, 2H), 7.81 (d, *J* = 7.3 Hz, 2H), 7.58-7.51 (m, 8H), 7.43-7.36 (m, 6H), 2.06-2.00 (m, 8H), 1.22-1.09 (m, 26H), 0.83-0.79 (m, 20H). <sup>13</sup>C{<sup>1</sup>H} NMR (100 MHz, CDCl<sub>3</sub>, δ): 151.13, 150.83, 141.32, 141.00, 139.86, 128.88, 127.25, 127.01, 126.99, 125.89, 125.50, 125.08, 123.02, 119.91, 119.68, 55.29, 40.54, 31.67, 29.87, 24.03, 22.72, 14.17. Anal. calcd for C<sub>60</sub>H<sub>72</sub>: C, 90.85; H, 9.15; found: C 90.88, H 9.22. MALDI-TOF-MS (*m/z*): calcd for C<sub>60</sub>H<sub>72</sub>, 792.563; found, 792.571.

**Table S1.** Absorption data for **1** and **2**.

Compound	Absorption <sup>a)</sup>
	$\lambda_{\text{abs}}$ [nm]
<b>1</b>	228, 275, 324
<b>2</b>	228, 272, 314

<sup>a)</sup>At a concentration of  $1.0 \times 10^{-5}$  mol/L in  $\text{CH}_2\text{Cl}_2$ .

**Table S2.** Emission lifetime for **1** and **2**.

Compound	$\tau$ [ns]	$\tau_{\text{average}}$ [ns] <sup>a)</sup>
<b>1</b>	$\tau_1 = 0.67$ (72.37%), $\tau_2 = 1.52$ (27.63%) (CH <sub>2</sub> Cl <sub>2</sub> )	0.90
	$\tau_1 = 0.83$ (77.10%), $\tau_2 = 1.90$ (22.90%) (film)	1.08
<b>2</b>	$\tau_1 = 0.67$ (73.49%), $\tau_2 = 1.76$ (26.51%) (CH <sub>2</sub> Cl <sub>2</sub> )	0.96
	$\tau_1 = 1.37$ (89.92%), $\tau_2 = 9.41$ (10.08%) (film)	2.18

<sup>a)</sup>  $\tau_{\text{average}} = \tau_1 \times X\% + \tau_2 \times (1-X)\%$ , where  $X\%$  is the percentage of  $\tau_1$ .

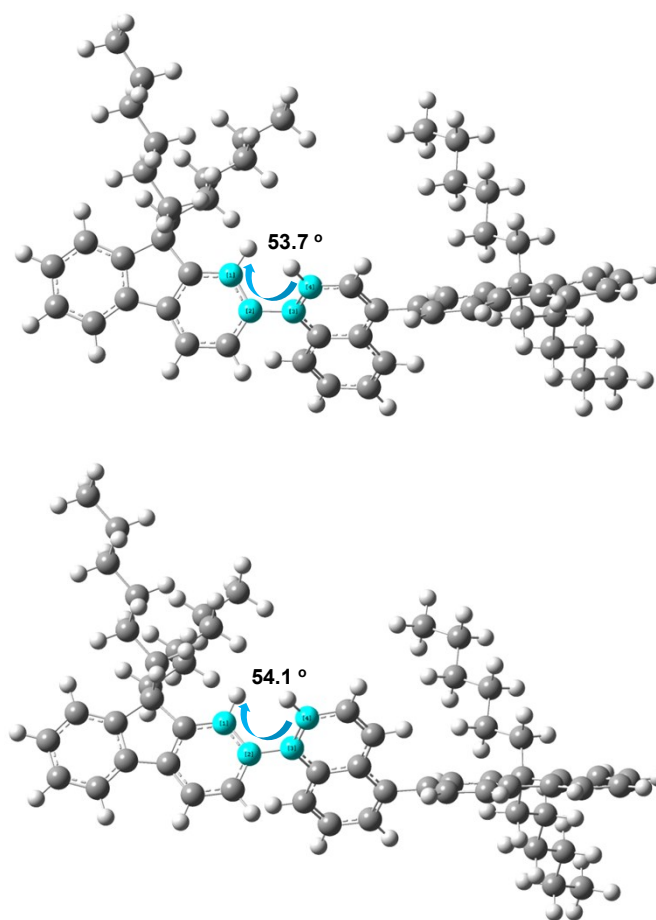


**Figure S1.** Calculated dihedral angles between fluorene and naphthalene moiety of **1** (up) and **2** (down) in the ground state.

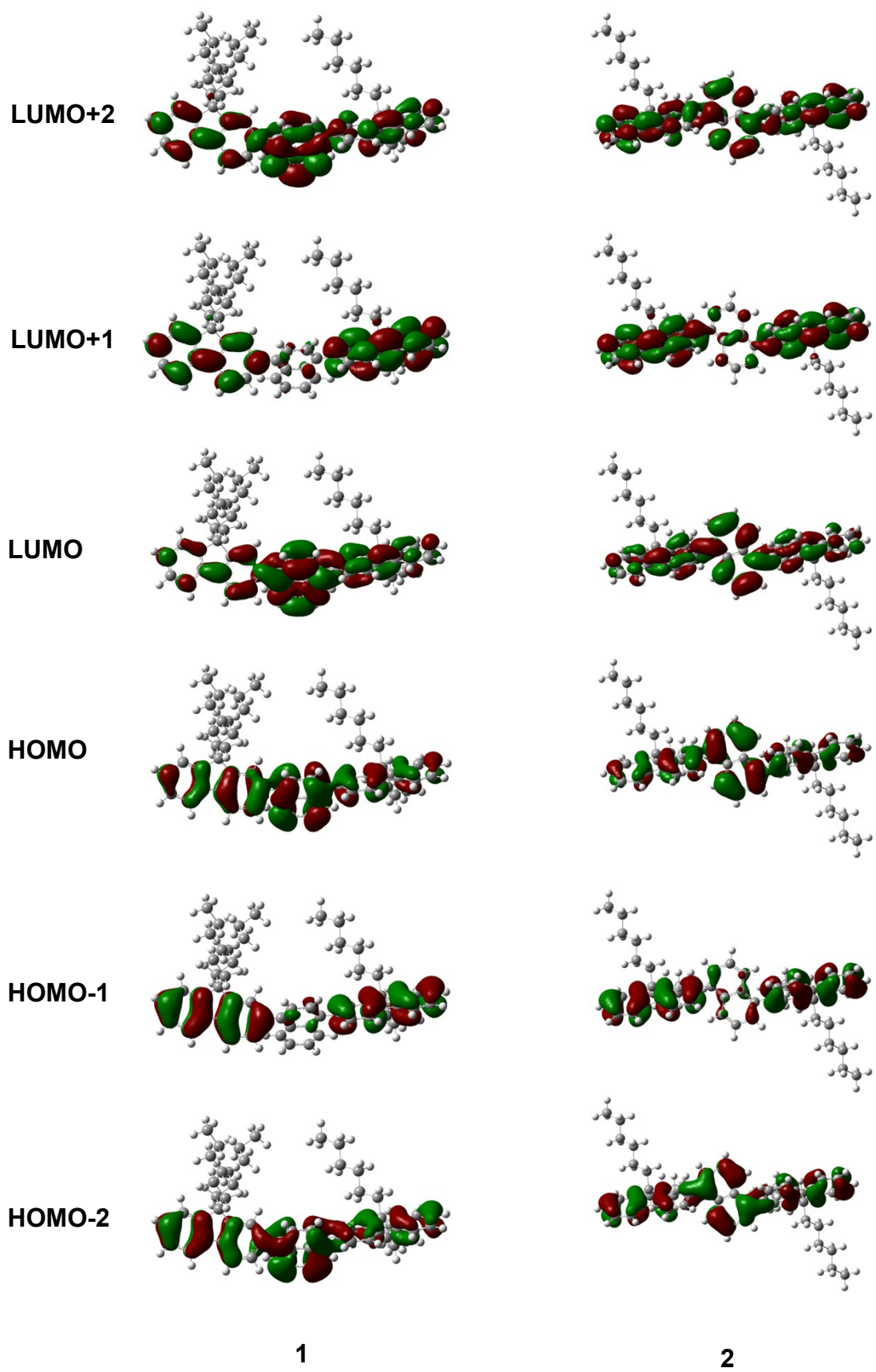


**Figure S2.** Calculated electron cloud distributions of selected molecular orbitals of **1** and **2**.



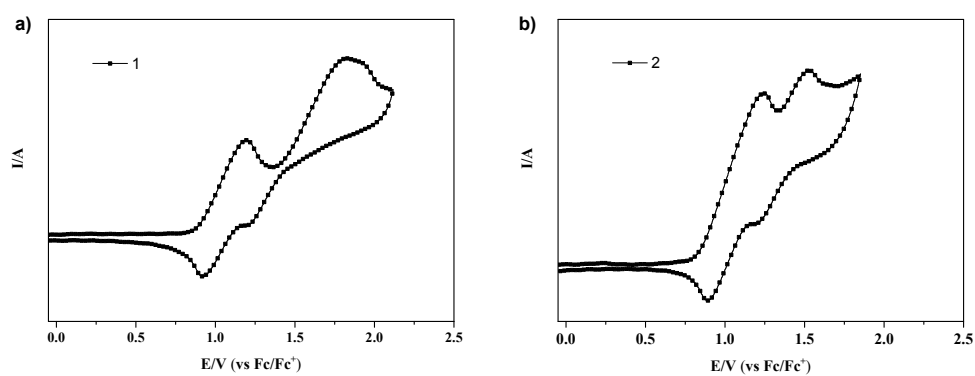


**Figure S3.** Cyclic voltammogram of **1** and **2** under a scan rate of 100 mV/s in CH<sub>2</sub>Cl<sub>2</sub>.

**Table S3.** Calculated energy levels for selected molecular orbitals of **1** and **2**.

	1	2
LUMO+2	-0.57662 eV	-0.50016 eV
LUMO+1	-0.75323 eV	-0.84466 eV
LUMO	-1.26835 eV	-1.22862 eV
HOMO	-5.27341 eV	-5.29382 eV
HOMO-1	-5.75452 eV	-5.69248 eV
HOMO-2	-6.01168 eV	-6.04406 eV

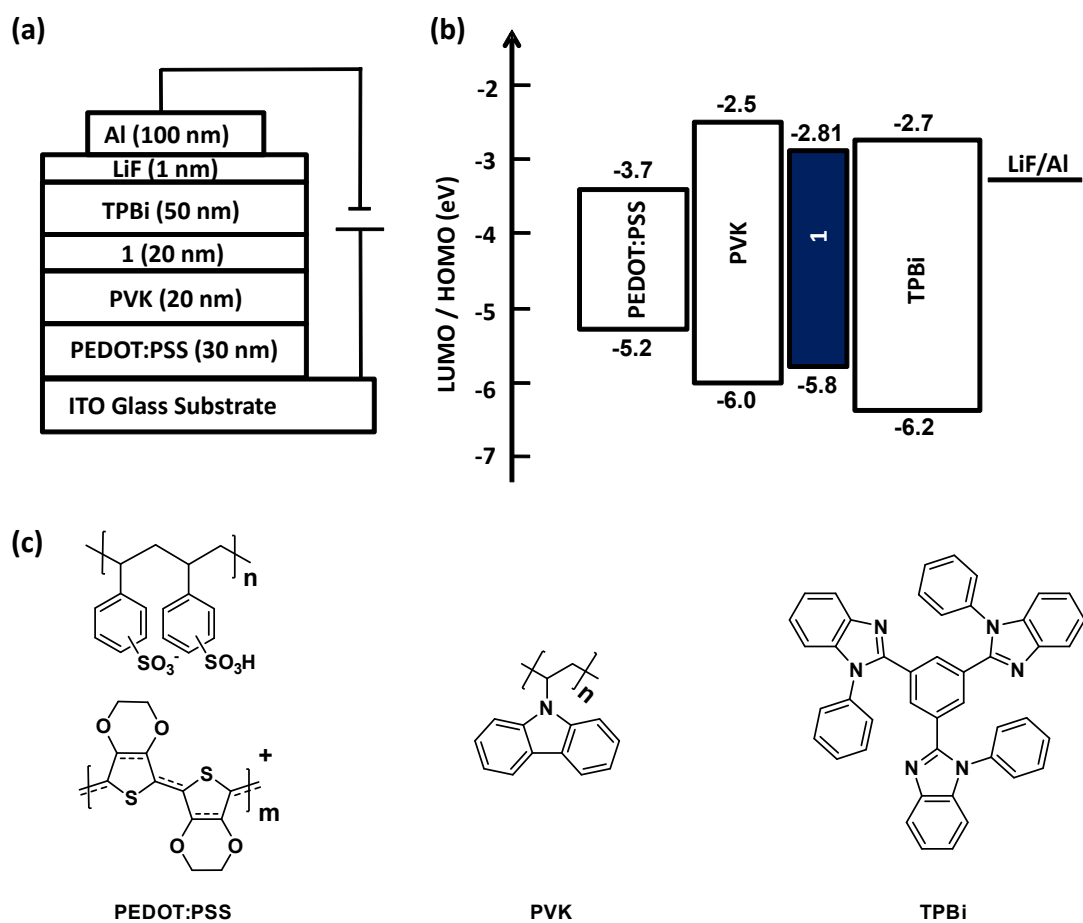


**Figure S4.** Device structure (a), schematic diagram of the energy levels (b) of the deep-blue OLED and chemical structures of the materials (c) involved in the fabricated devices.

**Table S4.** EL data for the deep-blue device based on **1**.

$\lambda_{\text{EL}}/\text{nm}$	CIE (x, y) <sup>a)</sup>	$V_{\text{ON}}^{\text{b)}}$ /V	$L_{\text{max}}/\text{cd}\cdot\text{m}^{-2}$	$CE_{\text{max}}/\text{cd}\cdot\text{A}^{-1}$	$PE_{\text{max}}/\text{lm}\cdot\text{W}^{-1}$	$EQE/\%$	FWHM/nm
410	(0.16, 0.08)	7	138	0.25	0.11	0.22	59
<sup>a)</sup> At	9	V;	<sup>b)</sup> Luminance	is	1	$\text{cd}\cdot\text{m}^{-2}$	

# NMR and MS Spectra

